OFFICE OF NAVAL RESEARCH

Grant or Contract N00014-96-1-0735

96PR05335-00

Technical Report No. 4

Single Polymer Chain Elongation by Atomic Force Microscopy

by

J. E. Bemis, B. B. Akhremitchev and G. C. Walker,

Prepared for Publication

in

Langmuir

University of Pittsburgh
Department of Chemistry
Pittsburgh, PA

1998

Reproduction in whole or in part is permitted for any purpose of the United States Government

This document has been approved for public release and sale; its distribution is unlimited

DTIC QUALITY INSPECTED 1

19980714 023

Single Polymer Chain Elongation by Atomic Force Microscopy

Jason Bemis, Boris Akhremitchev and Gilbert Walker * □
Department of Chemistry, University of Pittsburgh

*Author to whom correspondence should be addressed
□ 3M Untenured Faculty Awardee

Abstract

We have investigated the elastic deformation of single polystyrene-b-poly-2-vinyl-pyridine chains from spun cast films by Atomic Force Microscopy (AFM). A non-linear elastic response is shown to be present hundreds of nanometers above the bulk surface. The length of the elastic response monotonically increases with molecular weight of the polymer. These non-linear elastic responses are fit to wormlike chain (WLC) and freely joined chain (FJC) models giving persistence and Kuhn lengths of approximately 5 Å. The entropic models reveal that the polymer chains are stretched to 80-90% of their contour length before the attachment to the tip is ruptured.

Introduction

The understanding of adhesive properties of two surfaces in contact requires the detailed comprehension of the molecular interactions between the surfaces. This is necessary in numerous applications, from the agglutination of two surfaces, to the preparation of antifouling surfaces. Previous AFM studies of adhesion have focused on the intersurface properties from both experimental and theoretical standpoints.[1-6] Recent developments in AFM have allowed for the manipulation of single polymer chains,[7-11] providing an unprecedented opportunity to test molecular theories of adhesion. We have further developed the study of molecular adhesion, by investigating the interaction of a single commercial polymer chains between the tip of an AFM and the surface.

Figure 1 shows a schematic representation of polymer attachment to an AFM tip. If one or more chains are attached to the tip after the tip jumps free of the surface the tip will experience an adhesive force away from the surface until it breaks free from the polymer chains. AFM has been shown to be capable of elastically stretching single proteins when specific ligand-receptor pairs are used to bind the proteins to the tip.[11] Proteins have also been unfolded by reversibly attaching them to the tip.[10]

Entropic spring models of polymer chains have been used to explain polymer stretching.[10-12] The principal models considered here are the freely joined chain (FJC) and the wormlike chain (WLC). The FJC model predicts force-distance behavior described by the Langevin function, coth (β)-1/β, as shown by equation 1.

(1) $$F=(k\bullet T/A)\bullet(\coth(R)-1/R)$$

Where F is the tension between two points (nN), k and T are the Boltzmann constant (aJ/K) and temperature (K) respectively, A is the Kuhn length (nm), and R is the unitless extension ratio.

The extension ratio is the fraction of the polymer contour length that the chain is extended. If points A and B are separated by distance x, the extension ratio is x over the contour length of the chain between points A and B. The WLC model predicts a force-distance dependence described by equation 2.

(2) $$F=(k\bullet T/A)\bullet(0.25\bullet(1-R)^{-2}-0.25+R)$$

where A is now the persistence length (nm).

In this article, we report our examination of polystyrene-b-poly-2-vinyl-pyridine, which has been the focus of numerous studies.[13-19] The hydrophobic-hydrophilic block dynamics offers a wide range of applications, such as an interfacial bridge between immiscible homopolymers.[18] Models of adhesion between two surfaces in contact, such as JKR, are well developed, but fail to describe the appreciable adhesion when the surfaces are bridged by polymer chains.

Experimental

PS7800-P2VP10000, PS13800-P2VP47000, PS52400-P2VP28100, PS60100-P2VP46900, and PVP50000 were purchased from Polymer Source (Dorval, Canada) all with a polydispersity index less than 1.11 and were used without further purification. PS29100 was purchased from Aldrich with a polydispersity index of 1.04. Blocks are designated by PS for polystyrene and P2VP or PVP for poly-2-vinyl-pyridine. Molecular weights of the individual blocks are given after the designation for the block in units of Daltons. Block copolymers and polystyrene were dissolved in toluene (J.T. Baker) that was previously filtered with a 0.45μm nylon membrane. PVP was dissolved in THF (EM science); all solutions were approximately 2g/L.[20] Samples were prepared by spin casting onto 12mm diameter glass cover slips (Fischer Scientific) at 1000 RPM for 2 minutes using a Headway Research ED101D photo resist spinner.

All AFM measurements were conducted using a Digital Instruments (Santa Barbara, CA) Nanoscope IIIa Multimode scanning force microscope, typically in force volume mode. The spring constants were calibrated using a Park Scientific Instruments force constant calibration cantilever (Sunnyvale, CA), according to equation (3).[22]

(3) $$K=Kref\bullet(sensitivity-\delta_{test})/(\delta_{test}\bullet\cos\theta)$$

δ_{test} is the sensitivity (V/nm) on the reference standard, Kref=0.157 N/M, and theta is the angle of the cantilever in respect to the surface, taken as 11 degrees. Tip shapes were characterized by scanning a grating of 700 nm high, 20° cone angle, 10 nm radius tips (NT-MDT Moscow, Russia) to ensure minimal contamination of the tip. Tip radii we measure are typically on the order of 50 to 100 nm. All measurements were done in 0.45μm filtered 10mMol sodium acetate buffer using a Digital Instruments fluid cell. Sodium acetate was purchased from EM Science. Water was purified using a Barnstead NANO pure filter to 18 MΩ resistivity.

Force volumes of 16x16x512 points were collected using Nanoscope IIIa software and analyzed using custom software written for Matlab (Math Works Inc. Natick MA). Persistence lengths and maximum extension ratios were obtained from fitting elastic response curves to the WLC model and minimizing χ^2. Kuhn length and maximum extension ratios were obtained from fitting elastic response curves to an approximation[23] of the FJC model and minimizing χ^2. Relevant experimental scanning parameters are given in Table 1.

Contact angle measurements were conducted using a home built apparatus. The sample was housed in an environmental chamber continually flushed with humidified nitrogen. Images were collected using a CCD camera and video capture software. A Zisman plot of PVP50000 was constructed from a series of aqueous NaCl solutions 0, 5.43, 10.46, 14.92, 22.62, and 25.92% (w/w) (supporting information).

Results and Discussion

The surface topography of the block copolymers is irregular with sporadic height features on the order of 100 nm. There are ample areas (~1μm^2) which are devoid of height features greater than 15 nm. All force volume measurements were conducted in such areas so as to remove height aberrations from the force plots. There are small (~50 nm wide, 5 nm high) ordered structures, which may possibly be micellular in nature.[17] These features are not observed in air, although this may be due to the higher scanning forces induced by capillary forces. The topography of the homopolymer appears similar to the block copolymer, with the absence of the aforementioned structures. All samples were scanned in sodium acetate to decrease the force of adhesion by means of the double layer formed around the silicon nitride tip. This decrease in force of adhesion (1.7 nN to 1.1 nN) decreases the distance the tip travels when it jumps free of the surface, in turn increasing the distance over which data is obtainable.

Figure 2 represents a typical force plot in which an elastic response is observed. At point A in the retracting plot, the tip jumps free from the surface. It slowly goes to zero deflection until point B, 45 nm above the surface, where the tip begins to experience significant elastic tension from the attached polymer chain. At point C, 58 nm from the surface, the chain breaks free from the tip. This point is taken as the point of rupture, giving the length and force of the elastic response, 58 nm and 180 pN in this case. After this point the tip returns to zero deflection (point D) for the remainder of the z travel (360 nm).

Table 1 summarizes the statistical analysis of data collected. The lengths of the blocks are estimated from the covalent radii of carbon (0.77 Å), the C-C bond angle of 109.5°, and the number of monomers for the chain. The data represented in Table 1 is comprised of different types of elastic responses. The single elastic response shown in Figure 2 is the most frequent

response observed. Occasionally multiple elastic events are observed in a single force plot, as shown in Figure 3, which represent a smaller, but appreciable, content of the data. In rare cases, force plots are observed where the same chain is repeatedly strained as seen in Figure 4.

The elastic response of the polymer samples can be fit to both FJC and WLC models, as shown by Figure 2, the FJC being the dotted line. The statistical analysis of fitted values obtained from both models is summarized in Table 2. When the maximum extension ratio is a free parameter, the major difference in the two models is in the low force, low extension ratio regime (from 25 to 45 nm tip-sample separation in Figure 2). The noise in the data (10-20 pN standard deviation) at this low force, and the quality of the resulting fits to the two models precludes the choice of one model over the other, as demonstrated by χ^2 values. This is not entirely surprising as the WLC model requires only a small persistence length to fit the data well. The noise also results in shallow error functions for the persistence and Kuhn lengths.

We now examine the supposition that the majority of the elastic responses are the probing of one polymer chain. It is possible to estimate the number of chains between the tip and the surface based on the length and diameter. The diameter of the chain can be estimated from the Young modulus of the bulk and the persistence length.

(4) $$D=(32\bullet A\bullet k\bullet T/(\pi\bullet E))^{1/4}$$

Here D is the chain diameter, and E is the Young modulus (3 GPa for polystyrene). Figure 5 shows the persistence length and corresponding diameters for the multi-chain WLC fits. Kuhn lengths and corresponding diameters can be found in supporting information. The fourth root of the persistence length in equation 4 compensates for the large uncertainty of this parameter, so that the diameter of the chains have been accurately determined to be 2.5 Å ± 0.5 Å. This molecular scale diameter strongly suggests that a single chain is being extended, or that the chains

are being stretched in series.

An analysis of the length of the elastic response shows that it is unlikely that the chains being extended are in series. Figure 6 shows the length of the elastic response as the lower line, which is a linear increase with chain length with a slope of 0.2. The slope and its magnitude are presumably a consequence of chain entanglement. Longer chains are more likely to be entangled and the length to which they may be extended is proportionally smaller than the full length.[24] The upper line in Figure 6 is the estimated contour length of the chain between the tip and the surface based on the extension ratio obtained from the WLC fits. The estimated contour length is calculated by dividing the length of the elastic response by the maximum extension ratio. The extension ratios obtained with the FJC are higher, and so the estimated contour length of the chains based on that model will lie between the two lines shown. This estimated contour length of the chains is significantly less than the molecular weight-based estimate of the length of chains (Table 1). This discredits the interpretation that chains are being extended in series, in turn reinforcing our conclusion that most of the time a single chain is being stretched. The maximum length of the elastic response given in Table 1 shows that occasionally (~3%) there is an elastic response that exceeds the estimated length of the chains. This can be accounted for by the small amount of polydispersity.

We have also considered volume exclusion effects. In poor solvent conditions and low tension a polymer chain will collapse upon itself, forming a series of Pincus blobs.[25] This is particularly important at low extensions and has a predicted force-distance dependence as described by equation 5.[26]

(5) $$F \approx \gamma \bullet V^{1/2} \bullet D^{-1/2}$$

Where γ is the interfacial tension, V is the volume of the polymer globule that remains on the

surface, and D is the distance the chain has been pulled out of the globule. This behavior is apparent in Figure 2 from 15 to 25 nm tip sample separation. Our experiments were not optimized to collect data in this region of the force curve, but fits to equation 5 are reasonable. As this is the region in which volume exclusion effects are prevalent, we have ignored volume exclusion effects at higher extensions; regions of low tip sample separation and decreasing force with distance were not included in the fits to the elastic models.

Figure 3 shows multiple elastic responses in a single force plot. We consider two fundamentally different ways of explaining the origin of multiple elastic responses: from multiple chains or from multiple attachments of a single chain, schematically represented in Figure 1. For the case depicted in Figure 1a, there are two chains attached to the tip. Despite the low polydispersity of the samples, few chains will have identical contour lengths. Neither the length of the chain on the surface that is free from entanglement, nor the position of the tip attachment to the chain are required to be the same for each chain. The observed elastic responce will contain contribution from the elastic deformation of both the long and short chains.

In the case of a single chain with multiple attachments to the tip, the rupture of the first attachment exposes a greater contour length of the chain to stretching. In contrast to the multichain model, the rupture of this first attachment is independent of the elastic deformation of the second attachment.

Figure 3a was fit using the multichain model, and the individual elastic responses are shown as dotted lines above the sum. The multichain model yields higher persistence lengths and extension ratios than the single chain model for intermediate elastic responses.[27] As detailed in the caption of Figure 3, the intermediate responses have higher persistence lengths than those typically found.

The single chain and the multi-chain models are distinguishable by how well they fit multiple elastic responses to a single persistence or Kuhn length. For ease of discussion we will consider only the persistence length. When multiple elastic responses are fit by a single chain model the persistence lengths become very similar and can be fit quite well to a single persistence length for all of the elastic responses. In the example given in Figure 3b, a single persistence length of 4.4 Å gives a χ^2 of 0.59. The multi-chain, single persistence length fit (not shown) gives a 5.7 Å persitence length and a 0.76 χ^2 as the characteristic parameters, but fails to fit the intermediate responses. The persistence length of 4.4 Å for the single chain, single persitence length, corresponds to a diameter of 2.8 Å, further suggesting that even for multiple elastic responses in a single force plot a single chain is bridging the tip and the surface.

Based on the single chain model's success over the multi-chain, and the small persistence lengths obtained with both the FJC and WLC corresponding to small diameters of chains, we conclude that the majority of our data represents the elastic stretching of a single polymer chain. It then follows that the polymer chain is left on the surface, or else multiple chain dynamics would be observed for the majority of the force plots. However, it seems reasonable that if the chain is extended to lengths comparable to the length of the entire chain, one might suspect that the chain remains on the tip. Indeed, we have observed in rare cases (5 of 700+) entire force volumes (16x16 force plots) give rise to experimentally identical force plots over a lateral distance of a micron (data not shown). Each of these force plots exhibit the same elastic response, suggesting that there is indeed a single chain on the tip that is repeatedly stretched. This is not the case in most of the force plots, and suggests that the removal of a chain from the surface is a rare event.

In studies on titin, Gaub and coworkers showed that the multiple elastic responses were due to separate domains unfolding in a single chain.[10] Each domain unfolds under greater strain

than the previous, showing that multiple attachments of the chain to the surface or tip was not significant in the elastic response. This is obviously not the case in Figure 3, as the third elastic response ruptures under the least strain. In our study there are no rigid polymer domains along the length of the chain, consequently we identify elastic responses which detach additional polymer from the surface/tip, allowing weaker attachments to be exposed and rupture at different forces.

Figure 4 depicts three consecutively collected force plots. The top force plot shows the tip picking up a number of polymer chains. Subsequent force plots demonstrate the relaxation and stretching of the same group of chains. These particular force plots most likely involve multiple chains in series, as the tip-sample separation is approximately 282 nm.[28] The individual chains are estimated to be 192 nm, well below this length. The persistence length of 1.6 Å gives a diameter of 2.17 Å, suggesting that if indeed this force plots involves multiple chains they are in series. Of the approximately 200,000 force plots examined, these three are the only ones that demonstrate repeated stretching of polymer chains attached to the surface. If a z scan size is chosen that allows the tip to travel above the surface a distance comparable to the mean length of the elastic response, then the probability of repeatedly elongating the same polymer chains should increase. We are currently investigating further the reversibility of polymer chain stretching. It is also apparent that the force plots shown in Figure 4b and c exhibit elastic responses at the same tip-sample separations (100-150 nm).

The rupture force of the elastic response is determined by how well the polymer is attached to the tip, which in turn depends on the interfacial tension. There is no evidence of specific interactions between the tip and the chain, and so in principle the rupture force will allow for the distinction between blocks of a block copolymer. In an attempt to distinguish the blocks

that were studied here we conducted contact angle measurements on P2VP films. Linear regression of advancing contact angles of sodium chloride solutions gave a critical surface tension of 65.8 ± 0.7 dyne/cm. The Zisman plot can be found in the supporting information. Pure water gave a contact angle of 55 degrees, which through Young's equation gives an interfacial tension of 24.1 dyne/cm. Polystyrene has a surface energy of 33 dyne/cm [29] and a contact angle of 88 degrees [15] giving an interfacial tension of 30.5 dyne/cm. Assuming this similarity in interfacial tensions propagates to the interfacial tension of the polymer and the tip, this difference is beyond the accuracy of our force measurement.[30] In the case of PS-P2VP the difference in interfacial tensions of the two blocks with water are too close to distinguish. Using block copolymers with noticeably different interfacial tensions may allow for the distinction between polymer blocks, and possibly the mapping of surface segregation, as well as monitoring surface rearrangement as a function of solvent quality.

The dependence of the elastic response on contact time was studied on PS13800-P2VP47000 (Figure 7). Contact time was increased by increasing the maximum applied pressure while maintaining a constant z scan speed of 3300 nm/sec, and thus it is undetermined if the dependence is a function of contact time alone or if there is also an applied pressure component. Neither the rupture force of the elastic response nor the fitted values for the WLC and FJC model show a contact time dependence (Table 3, supporting material). However, there is a dramatic increase in the probability of an elastic response on increasing contact time (Table 3). It is also apparent that the relative probability of attaching a longer chain increases with contact time, as shown by the increase in average extension length of the elastic response (Figure 7). The upper line is the estimated contour length of the chain based on the maximum extension ratio from the WLC model. The increase in the average length of extension presumably results from an

improved attachment of the chain to the tip. This is no apparent dependence in the rupture force of the elastic event on contact time, as shown in Table 3 (supporting material).

Conclusions

We have demonstrated the ability of AFM to elastically extend a single polymer chain from a surface into the overlying solvent. We have shown that the WLC and FJC models fit the non linear elastic response with equal success. Persistence lengths so obtained indicate the chains have ca. 2.5 Å diameters, comparable to the estimated monomer size. The extension ratio obtained from the fits, the length of the elastic response, and the estimated contour length of the chains demonstrate that we are extending the polymer chains approximately 35% of their entire chain length. We first noted an elastic response in a random block copolymer with fluorinated side chains.[31] We now show this phenomenon to also be present in both homopolymer and block copolymer systems. AFM may serve as a useful tool to stretch single polymer chains in many other polymeric systems. The low force of this elastic response may be the reason that it is often unnoticed, but as lower forces are probed this phenomenon will need to be better understood.

Supporting Material Available: Table of contact time dependence on elastic chain model fits, Zisman plot, Kuhn lengths with corresponding diameters, histograms of maximum extension ratios for both WLC and FJC models, histograms of length of extension and force of extension for each of the polymers studied (3 pages). Ordering information is given on any current masthead page.

Acknowledgments

We would like to acknowledge ONR for financial support (N0001-96-1-0735).

References

(1) Aime, J. P.; Elkaakour, Z.; Odin, C.; Bouhacina, T.; Michel, D.; Curely, J.; Dautant, A. *J. Appl. Phys.* **1994**, *76*, 754-762.

(2) Burnham, N. A.; Colton, R. J.; Pollock, H. M. *Nanotechnology*, **1993**, *4*, 64-80.

(3) Hoh, J. H.; Cleveland, J. P.; Prater, C. B.; Revel, J. P.; Hansma, P. K. *J. Am. Chem. Soc.* **1992**, *114*, 4917-4918.

(4) Magonov, S. N.; Reneker, D. H. *Annu. Rev. Mater. Sci.* **1997**, *27*, 175-222.

(5) Sasaki, M.; Hane, K.; Okuma, S.; Bessho, Y. *Rev. Sci. Instrum.* **1994**, *65*, 1930-1934.

(6) Zhulina, E. B.; Walker G. C.; Balazs, A. C. *Langmuir*, in press.

(7) Chatellier, X.; Senden, T. J.; Joanny, J. F.; DiMeglio, J. M. *Europhysics letters* **1998**, *41*, 303-308.

(8) Florin, E. L.; Moy, V. T.; Gaub, H. E. *Science*, **1994**, *264*, 415-417.

(9) Noy, A.; Vezenov, D. V.; Kayyem, J. F.; Meade, T. J.; Lieber, C. M. *Chem. Biol.* **1997**, *4*, 519-527.

(10) Rief, M.; Gautel, M.; Oesterhelt, F.; Fernandez, J. M.; Gaub, H. E. *Science*, **1997**, *276*, 1109-1112.

(11) Rief, M.; Oesterhelt, F.; Heymann, B.; Gaub, H. E. *Science*, **1997**, *275*, 1295-1297.

(12) Marko, J. F.; Siggia, E. D. *Macromolecules*, **1995**, *28*, 8759-8770.

(13) Koneripalli, N.; Levicky, R.; Bates, F. S.; Ankner, J.; Kaiser, H.; Satija, S. K. *Langmuir*, **1996**, *12*, 6681-6690.

(14) Meiners, J. C.; Ritzi, A.; Rafailovich, M. H.; Sokolov, J.; Mlynek, J.; Krausch, G. *Appl. Phys. A* **1995**, *61*, 519-524.

(15) Parsonage, E.; Tirrell, M.; Watanabe, H.; Nuzzo, R. G. *Macromolecules*, **1991**, *24*, 1987-1995.

(16) Pelletier, E.; Stamouli A.; Belder, G. F.; Hadziioannou, G. *Langmuir*, **1997**, *13*, 1884-1886.

(17) Stamouli, A.; Pelletier, E.; Koutsos, V.; Vegte, E. V. D.; Hadziioannou, G. *Langmuir*, **1996**, *12*, 3221-3224.

(18) Shull, K, R.; Kramer, E. J.; Hadziioannou, G.; Tang, W. *Macromolecules*, **1990**, *23*, 4780-4787.

(19) Tang, W. T. Ph.D. Thesis, Stanford University, 1987.

(20) Static light scattering reveals that the CMC of PS-P2VP solutions in toluene is approximately 65μg/ml,[19] and as such, much of the work with PS-P2VP has been above the CMC. Adsorption of polystyrene-polyethylene oxide block copolymers from selective solvents above the CMC provide inhomogeneous film thickness and surface coverages.[21] However, the surface morphology of films made from toluene solutions of PS-P2VP block copolymers in the concentration range of 0.1 to 6 mg/ml are surprisingly uniform.[16] Part of the reason that the films are so homogenous, even when the film is made from a solution above the CMC, is that there is an appreciable concentration of unimers above the CMC.[19] Above 6 mg/ml there is a series of "worm-like"ridges.[16] By using solutions below this second critical concentration this morphology is avoided, simplifying the force-distance analysis.

(21) Munch, M. R.; Gast, A. P. *Macromolecules*, **1990**, *23*, 2313-2320.

(22) Tortonese, M.; Kirk, M. *Micromachining and Imaging*, **1997**, *3009*, 53-60.

(23) For extension ratios below 0.8 the inverse Langevin function was approximated by a 20th order polynomial. For higher extension ratios tan(R) was used.

(24) Wang, Y.; Winnik, M. A. *J. Phys. Chem.*, **1993**, *97*, 2507-2515, and references therein.

(25) Pincus, P. *Macromolecules*, **1976**, *3*, 386-388.

(26) Halperin, A.; Zhulina, E. B. *Europhysics letters*, **1991**, *15*, 417-421. Halperin, A.; Zhulina, E. B. *Macromolecules*, **1991**, *24*, 5393-5397.

(27) In both the single chain and multichain models the last elastic response is from one chain. This demands the same fitted values for the last response for both models. In Figure 3b (single chain model fit) the six elastic responses were fit to a single persistence length resulting in a slightly different result for the last response, than that of the multichain model used in Figure 3a.

(28) The vertical tip sample separation is 230 nm. With 125 nm of lateral offset between the first and third plot the total tip sample separation is 262 nm. The maximum extension ratio is 0.93 giving an estimated contour length of 282 nm.

(29) Israelachvili, J. *Intermolecular and Surface Forces*, 2nd ed.; Academic press: San Diego, 1992; pg. 204.

(30) The small amount of uncertainty in the sensitivity determination propagates to approximately 10% when using calibration standards of known force constants. As a result there does not appear to be a trend in the rupture force of the elastic responses, as shown in Table 1.

(31) Akhremitchev, B. B.; Mohney, B. K.; Marra, K. G.; Chapman, T. M.; Walker, G. C. *Langmuir*, **1998**, *14*, 3976-3982.

Figure 1 A: multichain model. When multiple elastic responses are observed, as in Figure 4, this model accounts for each response as a separate chain. This implies the entire elastic response of each chain is observed and that the force plot must be deconvoluted to determine the persistence or Kuhn length of each individual chain (as shown in Figure 4a). **B:** single chain model. Multiple elastic responses can also be explained by multiple attachments of a single chain from the tip and/or surface. This can be from multiple attachments on the tip/surface, where each rupture increases the fraction of the chain being stretched. The single chain model includes independent elastic responses, which results in lower and more consistent persistence and Kuhn lengths, when compared to the multichain model.

Figure 2 PS60800-PVP46900 collected with a 100 nm trigger, 500 nm z scan size and 1.95 Hz z scan rate. The upper dotted line is the advancing tip and the dashed line is the withdrawing tip. The solid line is a Wormlike Chain (WLC) fit to the elastic response observed after the tip jumped off the surface. The persistence length is 5.75 Å, maximum extension ratio 0.90 and χ^2 of 0.38. The lower dotted line is a Freely Joined Chain (FJC) fit to the same response with a Kuhn length of 5.86 Å, maximum extension ratio of 0.96, and χ^2 of 0.35. A, The tip jumps free of the surface. B, The tip elastically deforms a polymer chain still attached to the tip. C, The tip jumps free of the polymer chain, we often referred to this as the rupture point. D, the tip remains at zero deflection for the remainder of the scan.

Figure 3 PS60800-PVP46900 collected with a 100 nm trigger, 500 nm z scan size and 1.95 Hz z scan rate. **A:** The multi-chain, multi persistence length WLC fit is shown as the solid line with the individual responses shown as the thin dashed lines. From left to right the persistence lengths and maximum extension ratios are 0.19 nm and 0.75, 1.2 nm and 0.86, 2.2 nm and 0.88, 6.3 nm and 0.94, 2.1 nm and 0.92, 0.47 nm and 0.88. The fit gave a χ^2 of 0.321. **B:** Single chain fit with a single persistence length of 0.44 nm and χ^2 of 0.59. From left to right the maximum extension ratios are 0.86, 0.78, 0.73, 0.77, 0.84, 0.87. The solid line is the sum with the dotted thin lines as the individual responses.

Figure 4 PS52400-PVP28100 collected with a 100 nm trigger, 300 nm scan size, and at a scan rate of 1.95 Hz. All plots are sequential within the same force volume. There was 62.5 nm in lateral displacement between force plots. **A**: Force-distance plot showing the tip approaching the surface (dotted) and subsequently pulling out an entangled group of chains (dashed). **B**: Here the advancing tip reversibly relaxes the chains before they have detached from the tip. The solid line is a fit to the elastic responses using the WLC model. The fit gave a 0.91 maximum extension ratio and 1.2 Å persistence length C: Subsequent force plot showing the same process as B. WLC fit gave a 0.93 maximum extension ratio and 1.6 Å persistence length.

Figure 5 The solid line represents the persistence lengths obtained from multi-chain WLC fits to elastic responses. This histogram is the sum of all polymers studied as there is no noticeable difference in persistence lengths between molecular weights of block copolymers or homopolymers (see Table 2). The dashed line is the corresponding diameters to the persistence lengths.

Figure 6 Four molecular weights of PS-P2VP (see Table 1). The x axis is the polymer chain length, where the values are estimated from the molecular weights as described in the text. The lower solid line is the mean tip-sample separation at the rupture of the elastic response. The upper dashed line is the contour length of the chain between the tip and surface estimated from the maximum extension ratios obtained from the WLC model fits.

Figure 7 PS13800-PVP47000 z scan speed 3300 nm/sec. The lower solid line is the mean tip sample separation at the rupture of the elastic response. The upper dashed line is the estimated contour length of the chain based on the maximum extension ratios obtained from the WLC fits.

Table 1
summary of strand elongation length and force

polymer	length of blocks in nm [total length]	mean length of elastic response [nm]	maximum length of elastic response [nm]	median rupture force of elastic response [pN]	elastic event probability	relative trigger [nm]	z scan size [nm]	z scan rate [Hz]
PS7800-PVP10000	19/24 [43]	24.5	59.3	170 ± 40	0.30	50	130	4.88
PS13800-PVP47000	33/112 [145]	42.0	92.6	210 ± 30	0.03**	30	300	5.58
PS52400-PVP28100	126/67 [193]	44.5	94.1*	150 ± 25	0.52	100	300	1.95
PS60100-PVP46900	145/112 [257]	68.1	268.8	90 ± 14	0.24	100	500	1.95
PS29100	70	53.5	111.1	280 ± 30	0.22	100	300	4.88
PVP50000	119	65.2	125.6	120 ± 20	0.44	100	500	9.77

The elastic event probability is taken as the number of force plots exhibiting at least one elastic response divided by the total number of plots examined. The trigger is the maximum deflection exerted on the surface. Multiplying the trigger by the spring constant gives the maximum force exerted on the surface. The spring constants were approximately 0.07 ± 0.01 N/m except for the cantilever used on PVP, which was 0.03 N/m.

*force plots shown in Figure 4 were excluded from the maximum.

**Table 3 shows the dependence probability with contact time.

NOTE TO SCAN CONDITIONS: The scan conditions affect the observed elastic response. However, it was confirmed that the same conditions for different polymer weights did provide systematically different results. The final analysis assumes that the scan conditions play a minor role in the result, and as such the conditions were optimized for each molecular weight to decrease noise during scanning.

Table 2
Fitted parameters for the wormlike chain and freely joined chain models.

polymer	WLC			FJC		
	median persistence length Å	mean maximum extension ratio	mean χ^2	median Kuhn length Å	mean maximum extension ratio	mean χ^2
PS7800-PVP10000	3.0 ± 2.6	0.85 ± 0.04	0.70 ± 0.15	3.6 ± 2.7	0.94 ± 0.02	0.74 ± 0.17
PS13800-PVP47000	2.4 ± 2.1	0.85 ± 0.11	0.41 ± 0.26	3.0 ± 4.0	0.91 ± 0.08	0.49 ± 0.35
PS52400-PVP28100	2.9 ± 11.3	0.84 ± 0.08	0.40 ± 0.18	4.0 ± 11.6	0.94 ± 0.03	0.42 ± 0.18
PS60100-PVP46900	4.5 ± 14.0	0.83 ± 0.10	0.72 ± 0.44	5.8 ± 10.5	0.88 ± 0.18	0.70 ± 0.44
PS29100	3.7 ± 21.1	0.90 ± 0.05	0.57 ± 0.27	3.7 ± 6.4	0.96 ± 0.02	0.63 ± 0.27
PVP50000	4.0 ± 3.2	0.81 ± 0.07	0.25 ± 0.14	5.8 ± 2.8	0.91 ± 0.05	0.31 ± 0.18
All polymers	2.9 ± 10.5	0.82 ± 0.21	0.51 ± 0.30	3.8 ± 7.1	0.92 ± 0.09	0.56 ± 0.32

The maximum extension ratio is the ratio of the entire length of the chain between the tip and the surface divided by the distance at which the chain ruptures. ± values are standard deviation. All polymers represents all molecular weights of block copolymer and homopolymer studied.

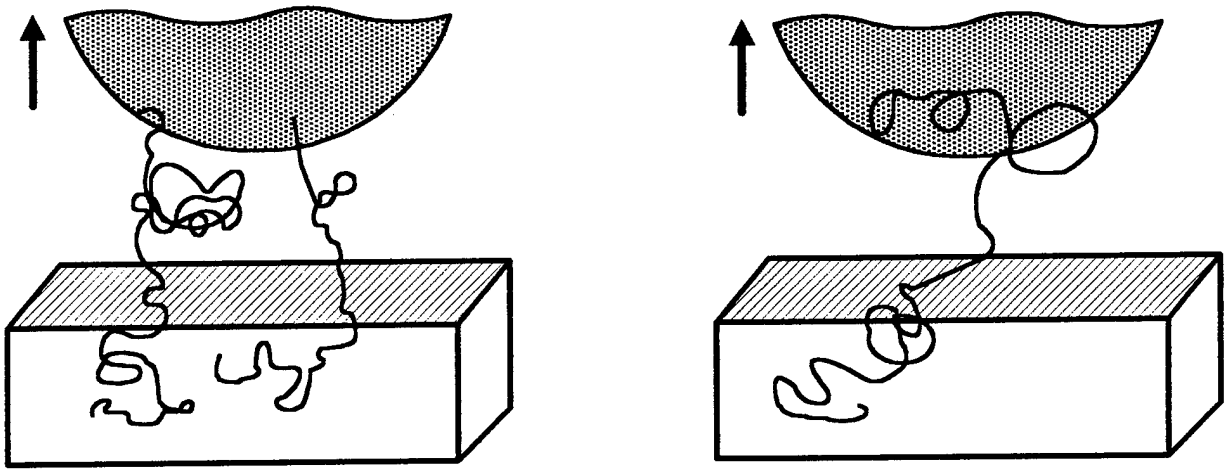

Figure 1

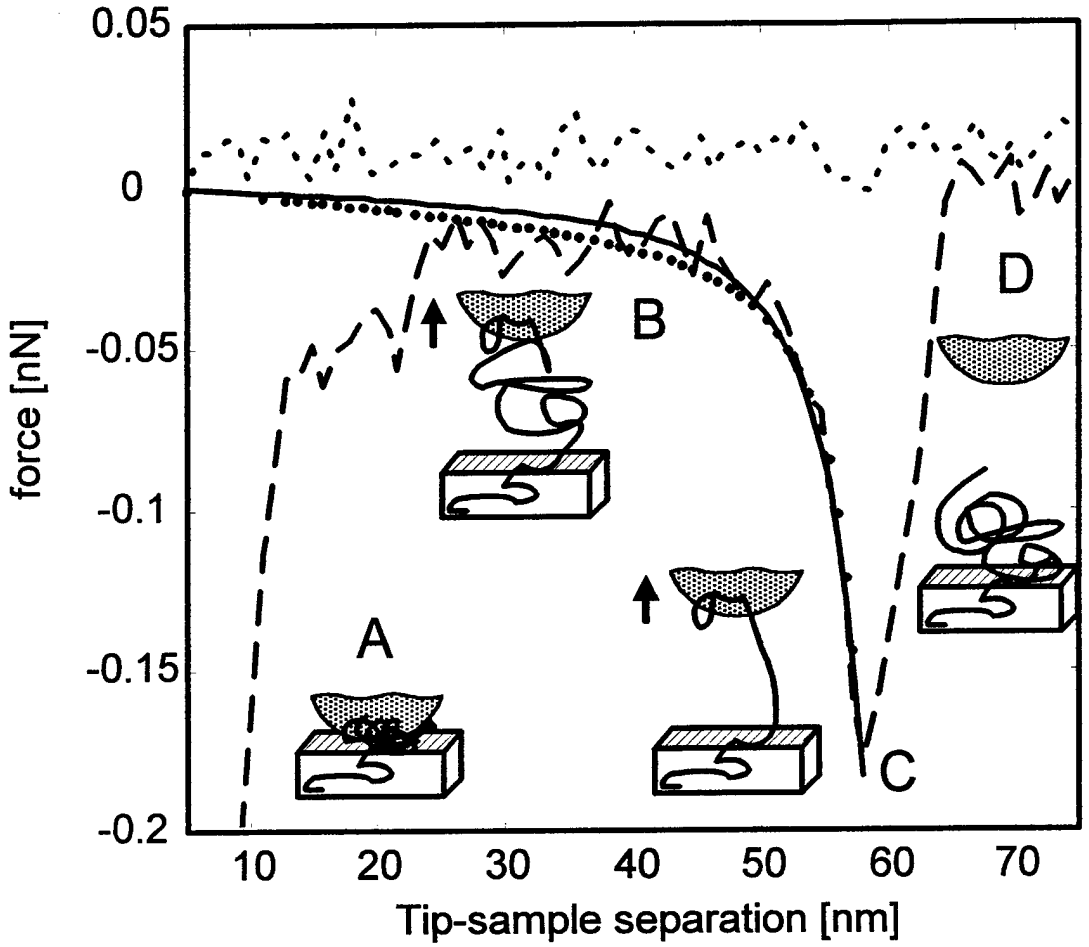
0.05
0
-0.05
-0.1
-0.15
-0.2
force [nN]
10
20
30
40
50
60
70
Tip-sample separation [nm]
A
B
C
D

Figure 2

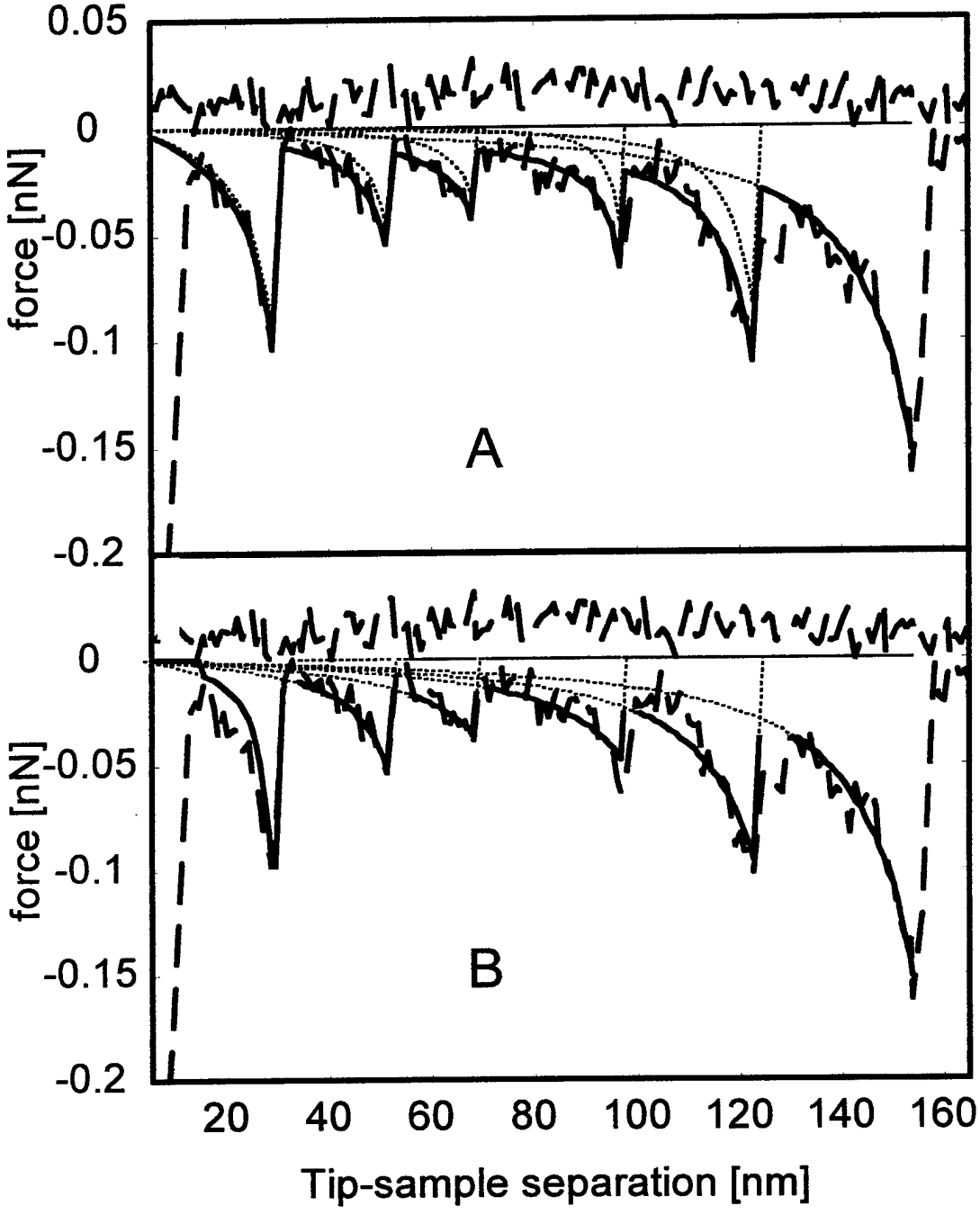
0.05
0
-0.05
-0.1
-0.15
-0.2
force [nN]
A
B
20
40
60
80
100
120
140
160
Tip-sample separation [nm]

Figure 3

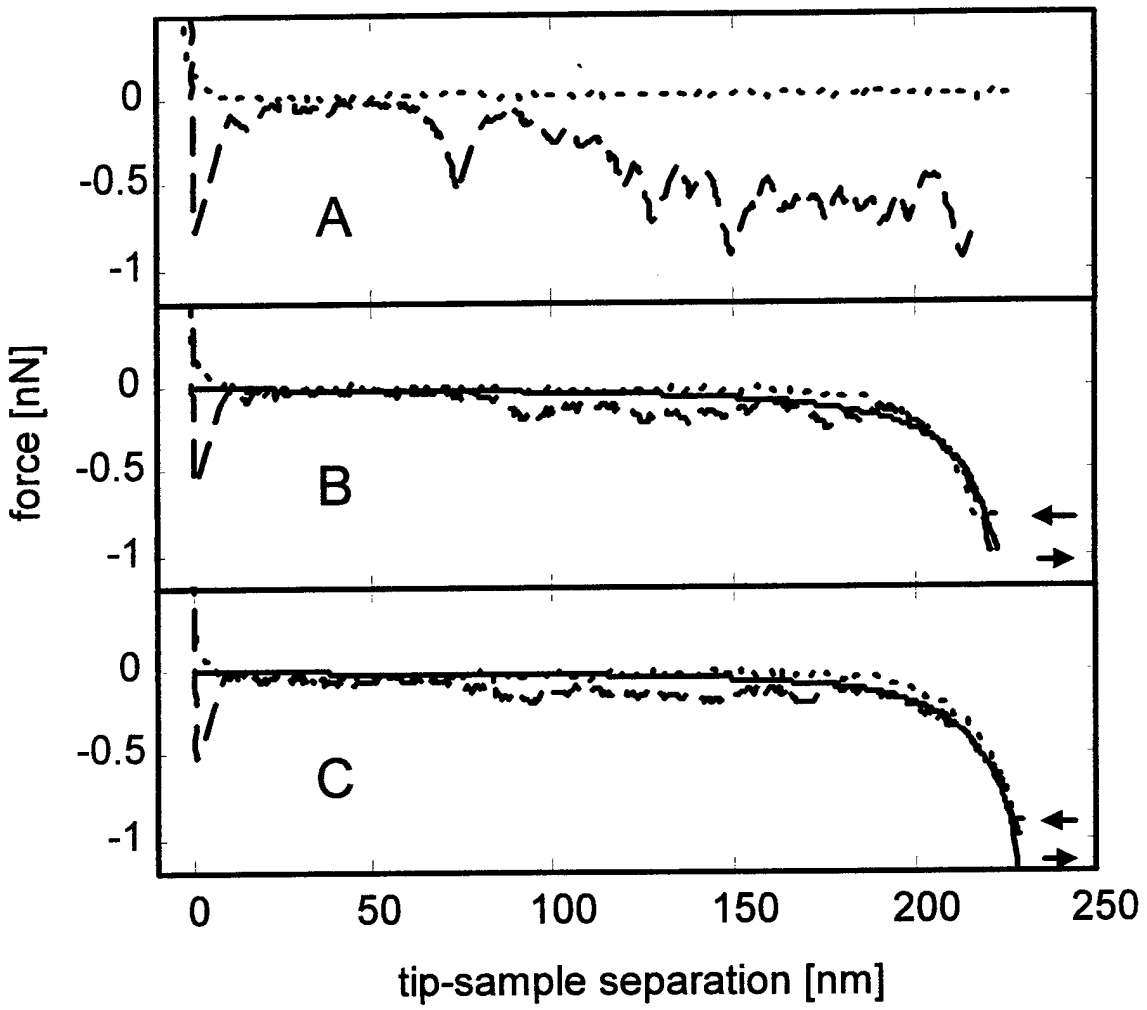
0
-0.5
-1
A
0
-0.5
-1
B
0
-0.5
-1
C
force [nN]
0
50
100
150
200
250
tip-sample separation [nm]

Figure 4

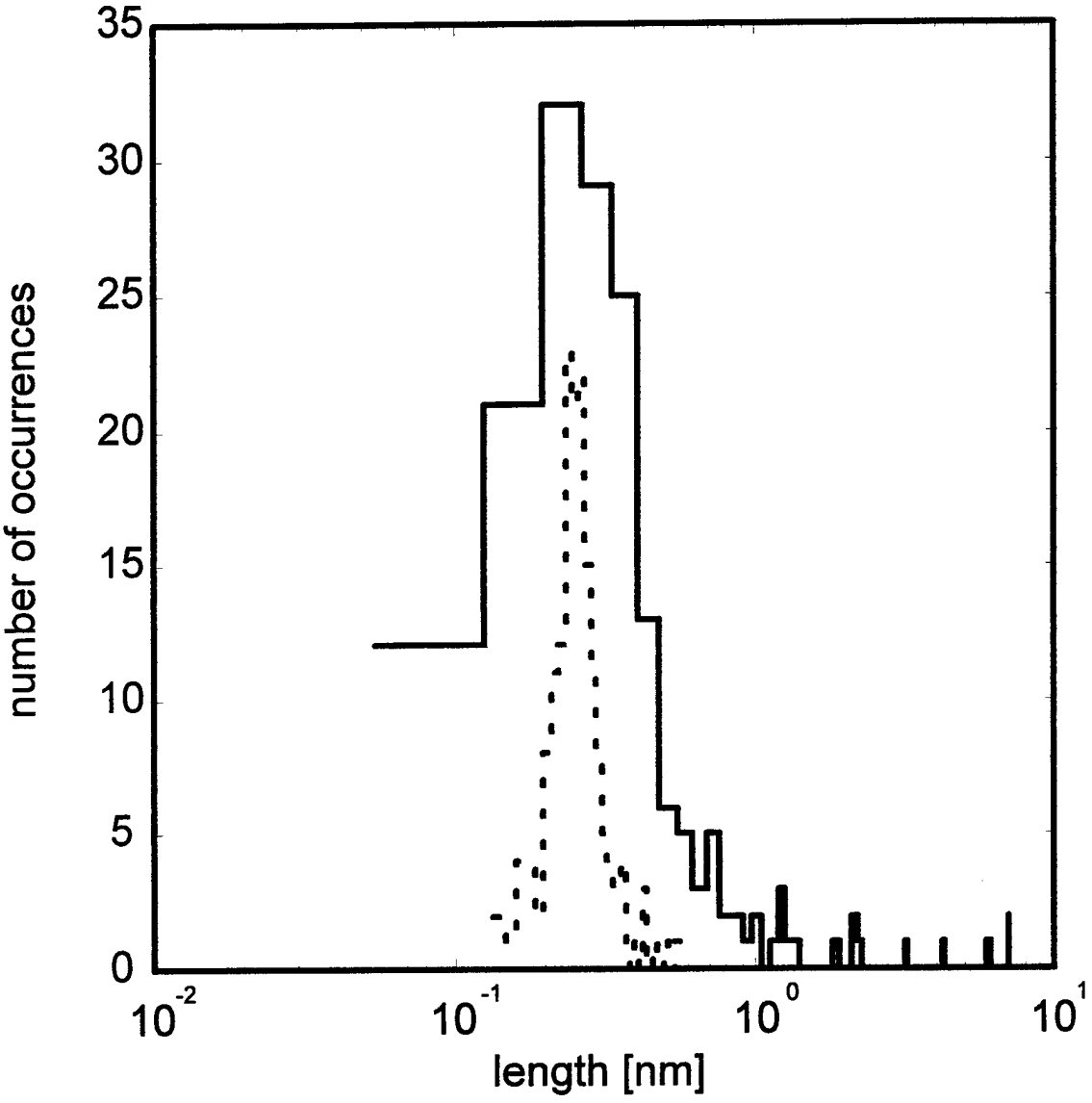
35
30
25
20
15
10
5
0
number of occurrences
10^{-2}
10^{-1}
10^{0}
10^{1}
length [nm]

Figure 5

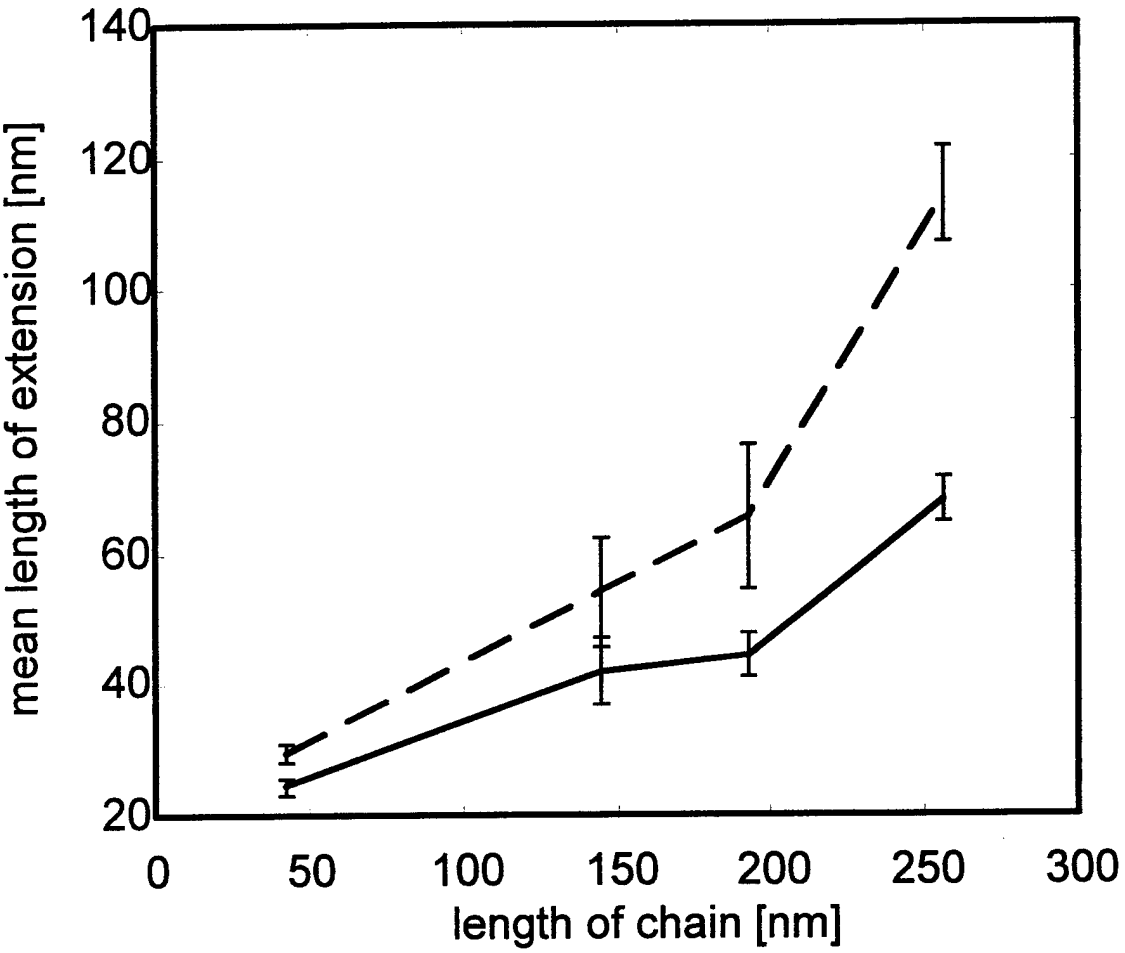
140
120
100
80
60
40
20
mean length of extension [nm]
0
50
100
150
200
250
300
length of chain [nm]

Figure 6

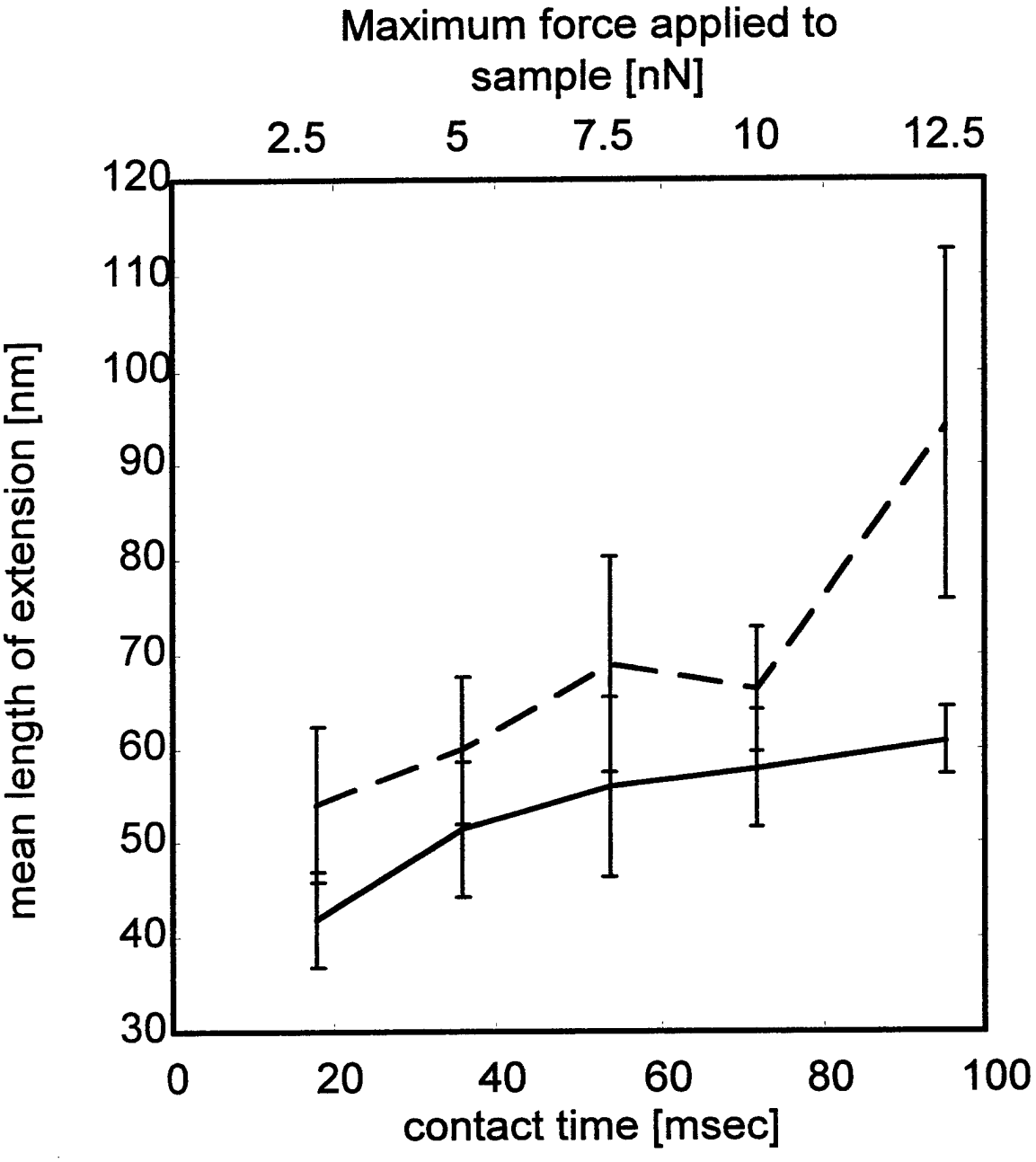
Maximum force applied to
sample [nN]
2.5
5
7.5
10
12.5
120
110
100
90
80
70
60
50
40
30
mean length of extension [nm]
0
20
40
60
80
100
contact time [msec]

Figure 7

Supporting material

Supporting 1: Zisman plot of poly-2-vinyl-pyridine 50000. Data (solid line and Xs) was obtained from 0, 5.43, 10.46, 14.92, 22.62, and 25.92% (w/w) NaCl solutions. Linear regression (dashed line) estimates the critical surface tension as 65.82 dyne/cm.

Supporting 2: The solid line represents Kuhn lengths obtained from FJC fits to elastic responses. This histogram is the sum of all polymers studied; there is no noticeable difference in Kuhn lengths between molecular weights of block copolymers or homopolymers. The dashed line shows the corresponding diameters for those Kuhn lengths.

Supporting 3: Histograms of maximum extension ratios. The histogram with the dashed peak to the right (~0.95) corresponds to the FJC model. The peak to the left (~0.87) corresponds to the WLC. These histograms are the sum of all polymers studies as there is no noticeable difference in maximum extension ratios between molecular weights of block copolymers or homopolymers.

Supporting 4: Histograms of the length of elastic response. The y axis is number of occurrences, with the label denoting the molecular weight of the polymer studied. The mean, maximum, and scan conditions are summarized in Table 1.

Supporting 5: Histograms of the force of elastic response. The y axis is number of occurrences, with the label denoting the molecular weight of the polymer studied. The median and scan conditions are summarized in Table 1.

Table 3
summary of contact time dependence on elastic responses

contact time [msec]		17.9	35.8	53.8	71.7	95.2	All times
maximum applied force [nN]		2.2	4.5	6.7	9.0	11.2	
Worm-like Chain	median persistence length Å	2.2 ± 1.0	1.9 ± 0.8	2.0 ± 0.9	2.5 ± 3.0	2.4 ± 1.9	2.3 ± 2.1
	mean maximum extension ratio	0.78 ± 0.17	0.85 ± 0.03	0.85 ± 0.03	0.81 ± 0.10	0.82 ± 0.08	0.85 ± 0.11
	mean χ^2	0.67 ± 0.36	0.47 ± 0.02	0.30 ± 0.18	0.35 ± 0.21	0.35 ± 0.20	0.41 ± 0.26
Freely Joined Chain	median Kuhn length Å	2.7 ± 1.2	2.9 ± 1.1	2.5 ± 0.92	3.8 ± 6.3	3.0 ± 2.2	3.0 ± 4.0
	mean maximum extension ratio	0.88 ± 0.13	0.94 ± 0.01	0.94 ± 0.02	0.91 ± 0.08	0.92 ± 0.05	0.91 ± 0.08
	mean χ^2	0.77 ± 0.48	0.56 ± 0.10	0.38 ± 0.28	0.36 ± 0.23	0.46 ± 0.32	0.49 ± 0.35
Median rupture force of elastic response [nN]		0.19 ± 0.02	0.34 ± 0.03	0.28 ± 0.02	0.18 ± 0.01	0.23 ± 0.01	
Probability of elastic response		0.03	0.04	0.05	0.08	0.17	

PS13800-P2VP47000. The maximum extension ratio is the ratio of the entire length of the chain between the tip and the surface divided by the distance at which the chain ruptures. ± values are standard deviation. All times represents the sum of all the contact times studied. Contact time was obtained by increasing the relative trigger while maintaining a constant z scan speed of 3300 nm/sec. The elastic event probability is taken as the number of force plots exhibiting at least one elastic response divided by the total number of plots examined.

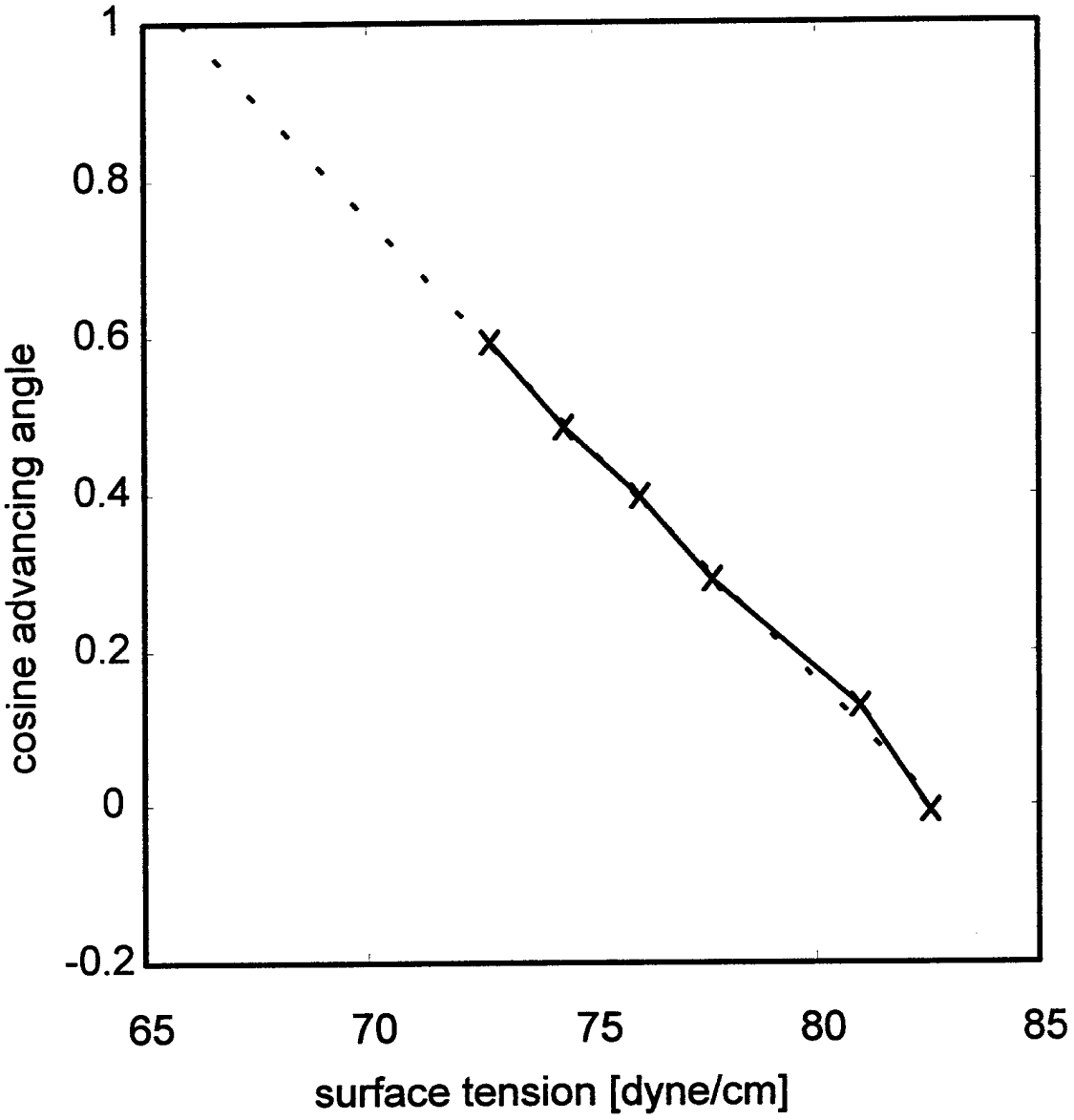

Supporting 1

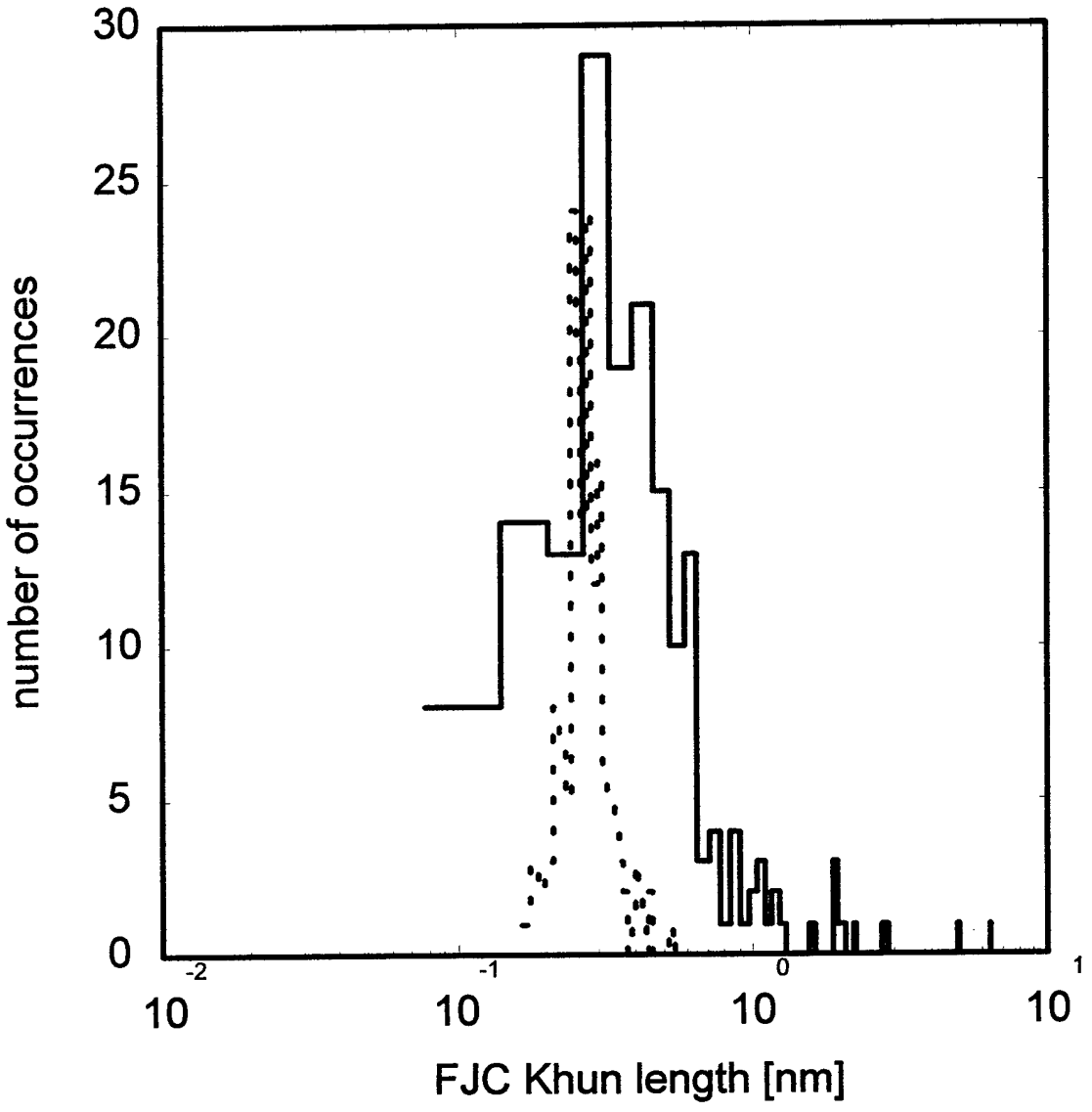

Supporting 2

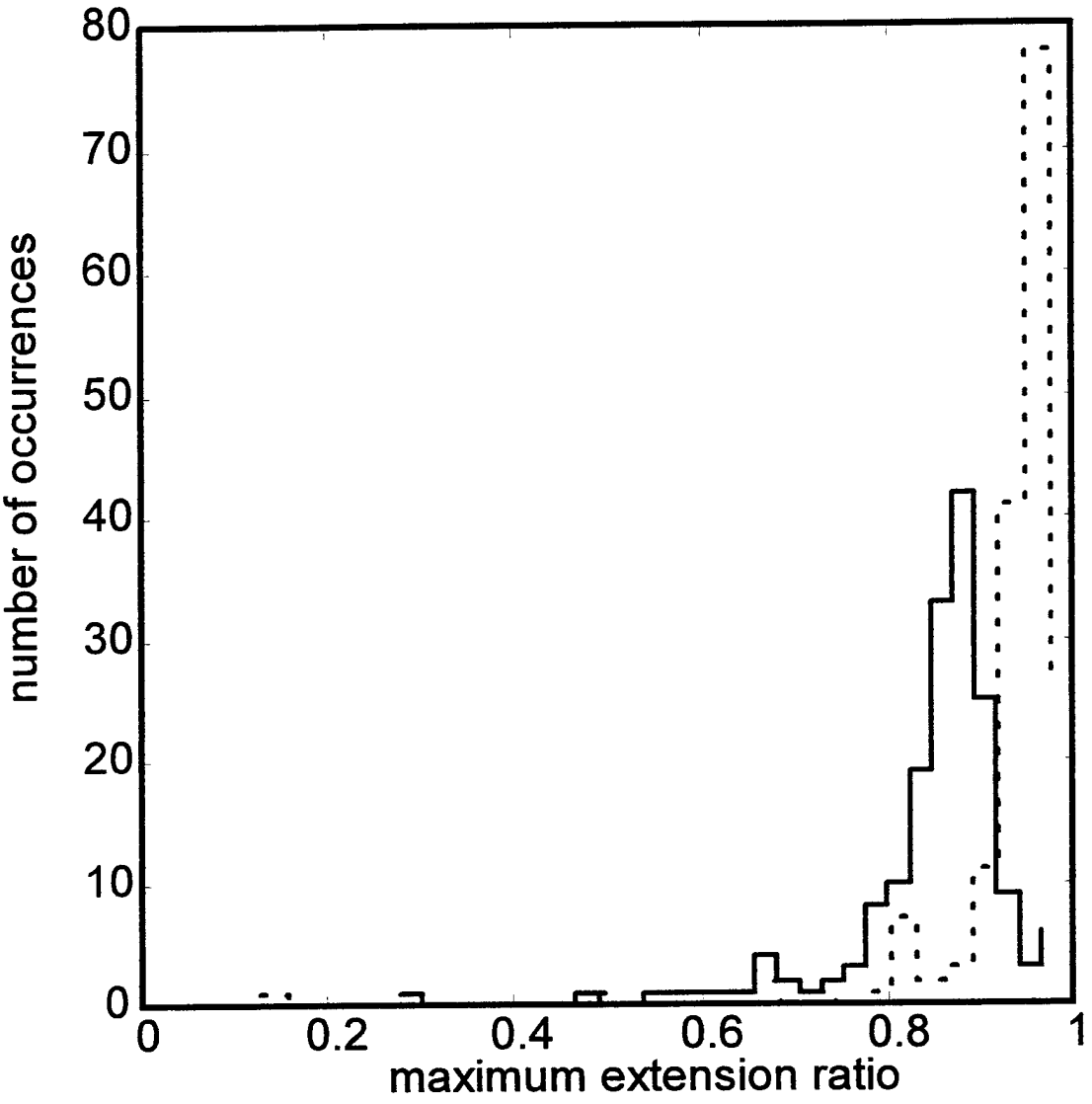

Supporting 3

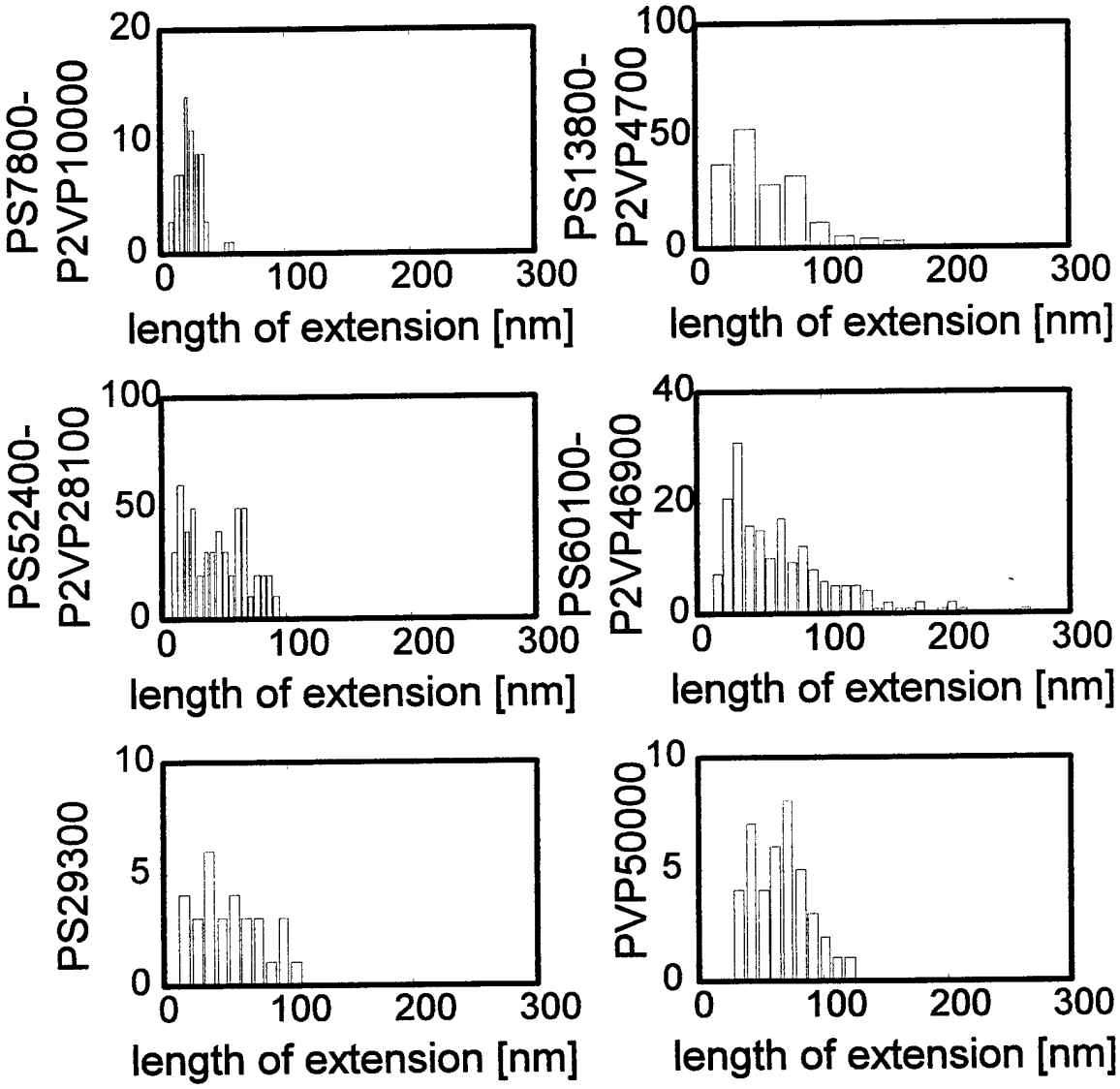

Supporting 4

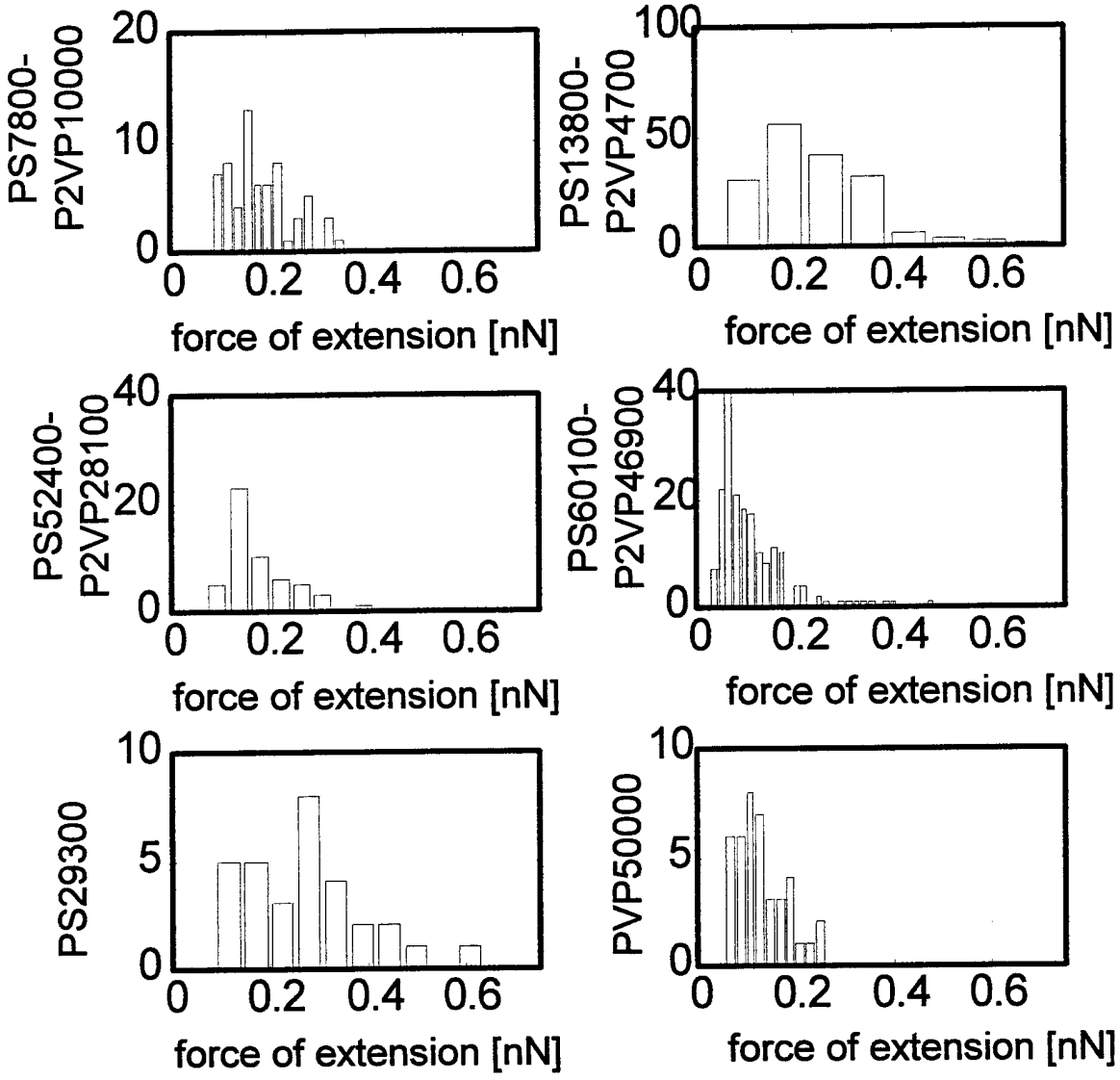

Supporting 5

REPORT DOCUMENTATION PAGE

Form Approved
OMB No. 0704-0188

Public reporting burden for this collection of information is estimated to average 1 hour per response, including the time for reviewing instructions, searching existing data sources, gathering and maintaining the data needed, and completing and reviewing the collection of information. Send comments regarding this burden estimate or any other aspect of this collection of information, including suggestions for reducing this burden, to Washington Headquarters Services, Directorate for information Operations and Reports, 1215 Jefferson Davis Highway, Suite 1204, Arlington, VA 22202-4302, and to the Office of Management and Budget, Paperwork Reduction Project (0704-0188), Washington, DC 20503.

1. AGENCY USE ONLY (Leave blank)	2. REPORT DATE	3. REPORT TYPE AND DATES COVERED
	July 1998	Technical

4. TITLE AND SUBTITLE
Single Polymer Chain Elongation by Atomic Force Microscopy

5. FUNDING NUMBERS
N00014-96-1-0735

6. AUTHOR(S)
Jason E. Bemis, Boris B. Akhremitchev and Gilbert C. Walker

7. PERFORMING ORGANIZATION NAME(S) AND ADDRESS(ES)
Department of Chemistry
University of Pittsburgh
Pittsburgh, PA 15260

8. PERFORMING ORGANIZATION REPORT NUMBER
98-4

9. SPONSORING / MONITORING AGENCY NAME(S) AND ADDRESS(ES)
Department of the Navy, Office of Naval Research
800 North Quincy Street, Arlington, VA 22217-5660

10. SPONSORING / MONITORING AGENCY REPORT NUMBER

11. SUPPLEMENTARY NOTES

12a. DISTRIBUTION / AVAILABILITY STATEMENT
This document has been approved for public release and sale, its distribution is unlimited.

12b. DISTRIBUTION CODE

13. ABSTRACT *(Maximum 200 words)*

We have investigated the elastic deformation of single polystyrene-b-poly-2-vinyl-pyridine chains from spun cast films by Atomic Force Microscopy (AFM). A non-linear elastic response is shown to be present hundreds of nanometers above the bulk surface. The length of the elastic response monotonically increases with molecular weight of the polymer. These non-linear elastic responses are fit to worm like chain (WLC) and freely joined chain (FJC) models giving persistence and Kuhn lengths of approximately 5Å. The entropic models reveal that the polymer chains are stretched to 80-90% of their contour length before the attachment to the tip is ruptured.

14. SUBJECT TERMS	15. NUMBER OF PAGES 34
	16. PRICE CODE

17. SECURITY CLASSIFICATION OF REPORT	18. SECURITY CLASSIFICATION OF THIS PAGE	19. SECURITY CLASSIFICATION OF ABSTRACT	20. LIMITATION OF ABSTRACT
Unclassified	Unclassified	Unclassified	UL